



Identification and functional prediction of long non-coding RNAs related to oxidative stress in the jejunum of piglets

Jinbao Li¹, Jianmin Zhang¹, Xinlin Jin¹, Shiyin Li¹, Yingbin Du¹,
Yongqing Zeng¹, Jin Wang^{1,*}, and Wei Chen^{1,*}

* Corresponding Authors:

Jin Wang

Tel: +86-15254817801,

E-mail: 15254817801@163.com

Wei Chen

Tel: +86-13695383461,

E-mail: wchen@sda.u.edu.cn

¹ Key Laboratory of Efficient Utilization of Non-grain Feed Resources (Co-construction by Ministry and Province), Ministry of Agriculture and Rural Affairs, Shandong Provincial Key Laboratory of Animal Biotechnology and Disease Control and Prevention, College of Animal Science and Technology, Shandong Agricultural University, Tai'an City, 271018, China

ORCID

Jinbao Li

<https://orcid.org/0009-0003-9647-4429>

Jianmin Zhang

<https://orcid.org/0000-0001-6428-5269>

Xinlin Jin

<https://orcid.org/0009-0005-8030-6281>

Shiyin Li

<https://orcid.org/0000-0002-3451-1912>

Yingbin Du

<https://orcid.org/0009-0009-3532-2580>

Yongqing Zeng

<https://orcid.org/0000-0002-0740-2470>

Jin Wang

<https://orcid.org/0000-0001-6974-4970>

Wei Chen

<https://orcid.org/0000-0002-2901-5156>

Submitted May 26, 2023; Revised Jul 18, 2023;

Accepted Jul 31, 2023

Objective: Oxidative stress (OS) is a pathological process arising from the excessive production of free radicals in the body. It has the potential to alter animal gene expression and cause damage to the jejunum. However, there have been few reports of changes in the expression of long noncoding RNAs (lncRNAs) in the jejunum in piglets under OS. The purpose of this research was to examine how lncRNAs in piglet jejunum change under OS.

Methods: The abdominal cavities of piglets were injected with diquat (DQ) to produce OS. Raw reads were downloaded from the SRA database. RNA-seq was utilized to study the expression of lncRNAs in piglets under OS. Additionally, six randomly selected lncRNAs were verified using quantitative real-time polymerase chain reaction (qRT-PCR) to examine the mechanism of oxidative damage.

Results: A total of 79 lncRNAs were differentially expressed (DE) in the treatment group compared to the negative control group. The target genes of DE lncRNAs were enriched in gene ontology (GO) terms and Kyoto encyclopedia of genes and genomes (KEGG) signaling pathways. Chemical carcinogenesis-reactive oxygen species, the Foxo signaling pathway, colorectal cancer, and the AMPK signaling pathway were all linked to OS.

Conclusion: Our results demonstrated that DQ-induced OS causes differential expression of lncRNAs, laying the groundwork for future research into the processes involved in the jejunum's response to OS.

Keywords: Jejunum; lncRNA; Oxidative Stress; Piglet; Transcriptome

INTRODUCTION

The term “oxidative stress” was first coined in 1985 [1]. Oxidative stress (OS) is defined as disruption of the prooxidant–antioxidant equilibrium, which leads to the production of reactive oxygen species (ROS) [2]. ROS are short-lived, strongly reactive oxygen-containing molecules that may harm DNA and change the DNA damage response [3]. ROS are crucial second messengers in many intracellular signaling cascades that try to keep the cell in equilibrium with its immediate surroundings. As ROS accumulate, OS occurs when the ROS level exceeds the maximum limit of the body's antioxidant defence system [4]. The intestinal barriers and intestinal cells are destroyed under OS conditions, leading to severe inflammatory bowel disorders and even bowel cancer. In ulcerative colitis, immune cells such as T cells cross the epithelial barrier, releasing inflammatory mediators and worsening mucosal damage [5,6]. Numerous elements in animal production can cause OS and damage cellular antioxidant defences. Weaned piglets may experience growth retardation, sickness, or even mortality as a result of OS [7]. Oxidative stress can result in subpar animal health, a decline in animal production efficiency, and significant financial losses in animal husbandry systems [8].

Homeostasis is maintained by cells through transcription and posttranscriptional regulation, which results in variations in gene expression [9,10]. lncRNAs are transcripts that are more than 200 nucleotides (nt) in length and lack an efficient open reading frame for translation. These transcripts typically regulate mRNA expression levels [11], nuclear organization [12], and diverse developmental processes such as differentiation [13]. lncRNAs serve critical functions in the cellular response to OS [14]. lncRNA NEAT1 is associated with H₂O₂-induced oxidative damage, and melatonin can attenuate H₂O₂-induced oxidative damage through the upregulation of lncRNA NEAT2 [15]. The lncRNA H19 is dramatically downregulated in the cochleae of old mice. In H₂O₂-stimulated HEI-OC1 cells, overexpression of H19 reduces mitochondrial ROS production and the apoptosis ratio. The mechanism is that lncRNA H19 protects cochlear hair cells from OS via the miR-653-5p/SIRT1 axis [16]. However, few lncRNAs induced by OS in the jejunum of piglets have been reported.

Diquat (DQ) is a fast-acting herbicide used to suppress terrestrial and aquatic plants as a contact and preharvest desiccant. Its ability to produce reactive oxygen and nitrogen species contributes to its toxic potential [17]. In addition to serving as an important agricultural and economic animal, the domestic pig (*Sus scrofa*) can serve as a model organism for medical research. Domestic pigs also produce a significant amount of meat for human consumption. Therefore, it is necessary to clarify the changes in lncRNA expression in piglets under OS. The purpose of this research was to explore lncRNAs related to OS between DQ-treated piglets and negative control (NC) piglets.

MATERIALS AND METHODS

Ethics statement

The animal study was reviewed and approved by the Animal Ethics Committee of Shandong Agricultural University, China, and performed in accordance with the Committee's guidelines and regulations (Approval No.: 2004006).

Experimental design and data collection

The experimental design and data for this study were obtained from our previous research [18]. The experimental design was as follows: 12 male Landrace piglets weaned at 21 days were collected and divided into the OS group and the NC group. In the OS group, piglets were intraperitoneally injected with DQ (Sigma-Aldrich, Saint Louis, USA) at 10 mg/kg body weight, while the NC group received an equivalent volume of isotonic saline. The trial lasted for seven days. Three piglets were selected from both the OS group and the NC group. After slaughter, the jejunum tissues were collected. Raw data with SRA number PRJNA661634 were downloaded

with sratoolkit (v3.0.0). Six samples (three from the OS group and three from the NC group) from this dataset were used for this study. Of these, L01, L02, and L03 were the NC samples, and L04, L05, and L06 were the OS samples.

Quality control for raw reads

The raw reads were quality-controlled before read alignment. Fastp (v0.23.2) [19] was used to filter the raw reads further. The reads with adapters, reads with unknown sequences, and low-quality reads were removed for quality control.

Read alignment, assembly and quantification

Sequencing reads were aligned using HISAT2 (v2.2.1) [20] against the reference genome (*Sus scrofa*.*Sscrofa*1.1.1.106.chr.gtf). To predict lncRNAs, the reads were then assembled and merged using StringTie (v2.2.1) [21]. Transcript expression levels were calculated for each sample using FeatureCounts (v2.0.3) [22] to obtain the gene counts. To reflect the expression levels of transcripts more realistically, the fragments per kilobase of transcript per million fragments mapped (FPKM) values were used as measures of transcript expression as calculated by Rstudio (v4.1.3).

Identification of lncRNA

The lncRNAs were screened according to their characteristics. Briefly, the merged transcripts were compared by GffCompare (v0.12.6) [23] with the *Sus scrofa* reference genome. i) Transcripts with class_code “i” (fully contained within a reference intron), “u” (intergenic), “x” (exonic overlap on the opposite strand), “o” (other same strand overlap with reference exons), “j” (multi-exon with at least one junction match) were selected. ii) Those transcripts that were more than 200 nucleotides in length and had an exon number greater than or equal to 2 were further considered for the identification of novel lncRNAs. iii) CPC2 (v3.0) [24] and CNCI (v2.0) [25] were used to identify whether the transcript is encoded. When the score <0, the transcript was considered incapable of encoding. The transcripts that were able to be compared to the Pfam [26] database were transcripts with a certain protein domain; they were considered to have coding ability, while the transcripts that were incomparable were considered potential lncRNAs. The criterion for Pfam domain screening was an E-value <1×10⁻⁵. Transcripts with an E-value >1×10⁻⁵ were screened and retained. iv) Those transcripts with FPKM >0.1 were retained for the identification of novel lncRNAs. The identification of novel lncRNAs was considered complete after the above screening. The merged transcripts of the six samples were annotated to the *Sus scrofa* genome to obtain known lncRNAs.

Differential expression analysis

DESeq2 [27] (v1.34.0) was employed for performing the dif-

ferential expression analysis based on the counts of genes in samples with biological replicates. Upregulated genes showed higher expression levels in the OS group compared to the NC group in the current study, whereas downregulated genes exhibited lower expression levels in the OS group compared to the NC group. Differentially expressed (DE) lncRNAs were defined as genes with a false discovery rate <0.05 and $\log_2(\text{fold change}) \geq 1$.

Target gene prediction of differentially expressed lncRNAs

Bedtools [28] (v2.30.0) was used to identify cis-target genes for DE lncRNAs. Neighbouring genes within 100,000 bp of DE lncRNAs were considered cis-target genes of the lncRNAs [29]. The Pearson correlation coefficient method [30] was used to predict trans-target genes. When the sample size was greater than or equal to six, the Pearson correlation coefficient method was used to analyse the correlation between lncRNAs and protein-coding genes among samples. Then, lncRNA-mRNA gene pairs with absolute correlation values ($|\text{cor}| > 0.95$ and $p < 0.05$) were retained.

Enrichment analysis of target genes

To further understand the function of DE lncRNAs, the gene ontology (GO) and Kyoto encyclopedia of genes and genomes (KEGG) databases were used for enrichment analysis of target genes of DE lncRNAs. The GO database contains three main categories of functional information: the biological processes, molecular function, and cellular component categories. Each of these categories contains a hierarchical network of terms that describe different aspects of gene function. KEGG provides pathway maps, gene annotations, and other related information to study the functions of genes within specific pathways. The target genes were then uploaded into the DAVID [31] database 2021. GO terms and KEGG pathways with $p < 0.05$

were considered significant by the DAVID database. To obtain the circos plot, the DAVID results were submitted to SangerBox (3.0).

Alternative splicing analysis

The pre-mRNAs transcribed from genes can undergo various splicing events, where different exons are selected to generate diverse mature mRNAs. These mature mRNAs are then translated into different proteins, contributing to the diversity of biological traits. ASprofile [32] was used to classify 12 types of alternative splicing (AS) events for each sample.

Quantitative real-time polymerase chain reaction analysis

Six DE lncRNAs were randomly selected to verify whether their expression was consistent with the trends of the RNA-seq results. Total RNA was extracted from piglet jejunal tissues using TRIzol (Invitrogen, Carlsbad, CA, USA). An Agilent 2100 Bioanalyzer (Agilent Technologies, Santa Clara, CA, USA) was employed to assess RNA quality. The cDNA was then synthesized. For the relative quantification of lncRNA, glyceraldehyde-3-phosphate dehydrogenase (GAPDH) was employed as an internal reference gene. Primers of selected lncRNAs (Table 1) were designed and then synthesized by Accurate Biotechnology Co., Ltd, Changsha, China. The quantitative real-time polymerase chain reaction (qRT-PCR) system for lncRNA had a total volume of 20 μL . The system consisted of 10 μL of 2X SYBR Green Pro Taq HS Premix, 0.4 μL of forward primer, 0.4 μL of reverse primer, 2 μL of cDNA template, and 7.2 μL of RNase-free water. Run the formulated 20 μL system on a Light Cycler 96 real-time PCR system (Roche, Basel, Switzerland) with the following program: 95°C for 30 s followed by 40 cycles of 95°C for 5 s and 60°C for 30 s. The $2^{-\Delta\Delta\text{CT}}$ relative quantification approach [33] was utilized to perform the quantitative analysis of the

Table 1. Primers for quantitative real-time polymerase chain reaction analysis

Gene	Sequence (5'-3')	Chromosome number	Genomic position
GAPDH-F	AAGTTCCACGGCACAGTCAAG		
GAPDH-R	CACCAGCATCACCCCATTT		
MSTRG.13992.1-F	GAATGTGCTGTCCTCTCCCTTA	6	169769542-169774327
MSTRG.13992.1-R	CCTCTATCCTGTGGCTTCATCTAC	6	169769542-169774327
ENSSSCG00000051217-F	TCTCCTGGCAAGGTGAGAAGC	14	85421568-85426434
ENSSSCG00000051217-R	CATTGCCCGATGCCAGAGAAC	14	85421568-85426434
ENSSSCG00000042863-F	CCTGGAACCTCTGGGAAACAGGA	5	56447575-56451669
ENSSSCG00000042863-R	CCCCTGAAGCCATTCAGCTCT	5	56447575-56451669
ENSSSCG00000046347-F	ACCCATGTGTTGCCAAAACACTACC	14	67559596-67576058
ENSSSCG00000046347-R	TCTCTCCCAAGCATTAGTCTGGA	14	67559596-67576058
ENSSSCG00000048058-F	TTTCAGCAGGCACCACACTCT	9	123345691-123457331
ENSSSCG00000048058-R	CCTGTGCCACCAAGACTGAGA	9	123345691-123457331
ENSSSCG00000042361-F	AGACAATGTTCTGCGAAGAA	15	3113891-3179365
ENSSSCG00000042361-R	GCCTCAGTCCATCCTCTCATA	15	3113891-3179365

GAPDH, glyceraldehyde-3-phosphate dehydrogenase; F, the forward chain of primers; R, the reverse chain of primers.

data.

RESULTS

Overview of the sequencing data

The GC content of each sample was greater than 50.28%, Q20% was above 97.71%, Q30% was above 93.50%, and N% was below 0.01% after quality control (Table 2). This indicated that the clean reads obtained were suitable for subsequent transcriptome analysis. In total, 95.33% to 96.67% of the clean reads of individual samples were mapped to the *Sus scrofa* reference genome. A total of 84.05% to 87.18% of the mapped reads were considered unique mapped reads, while only 4.96% to 7.18% of the mapped reads were multiple mapped reads (Table 3). The mapping results indicated that the quality and reliability of the sequencing data were relatively high.

Filtering of lncRNAs

Overall, 78,398 transcripts were used as input. A total of 790 candidate novel lncRNAs were finally identified (Figure 1A). A total of 13,053 transcripts were kept by filtering and retaining transcripts with class_codes "i", "u", "x", "o", "j". A total of 83.35% of the initial transcripts were filtered; this was the step that filters out the most transcripts in identifying novel lncRNAs. After removing transcripts that were less than 200 nt in length and had an exon numbers less than 2, 12,702

transcripts remained. Only 0.48% of transcripts were further filtered out in this process. A total of 2,486 transcripts were retained through CNCI filtering; 2,162 transcripts were retained through CPC2 filtering; and 2,138 transcripts were retained through Pfam protein structural domain analysis. The results of the three software programs were intersected, and 1,179 transcripts were preserved (Figure 1B). A total of 9.07% of transcripts were further filtered out in this process. Transcripts with low expression were then removed. A total of 0.49% of transcripts were further filtered out in this process. Finally, 790 transcripts were retained. The 790 transcripts obtained were considered to be novel lncRNAs. The merged transcripts were compared with the *Sus scrofa* reference genome, and the transcripts with low expression were removed, resulting in 5,289 known lncRNAs. Ultimately, a total of 6,079 lncRNAs were identified.

Genomic characterization of lncRNAs

The exon number distribution statistics of lncRNAs showed that the highest number of exons was 1, 2 (Figure 1C). Most lncRNAs were distributed on chromosome 1 in jejunal tissue, followed by chromosome 6 and chromosome 13 (Figure 1D). The length distribution statistics of lncRNAs showed that the most common length bin of the lncRNAs in the samples was 3,001 nt to 6,000 nt, followed by 200 nt to 3,000 nt and 6,001 nt to 9,000 nt (Figure 1E).

Table 2. Statistics of sequencing read quality control

Sample	L01	L02	L03	L04	L05	L06
Total reads count (#)	168,319,300	204,605,264	184,167,668	110,986,482	114,567,750	106,287,400
Total bases count (bp)	25,099,860,074	30,490,139,350	27,525,906,846	16,589,901,748	17,103,222,848	15,880,642,184
Average read length (bp)	149	149	149	149	149	149
Q20 bases count (bp)	24,591,604,302	29,804,193,516	26,896,425,748	16,305,157,015	16,796,443,609	15,526,006,867
Q20 bases ratio (%)	97.76	97.75	97.71	98.28	98.20	97.76
Q30 bases count (bp)	23,496,831,051	28,543,214,436	25,737,842,587	15,749,508,935	16,207,042,479	14,875,967,073
Q30 bases ratio (%)	93.61	93.61	93.50	94.93	94.76	93.67
N bases count (bp)	15,482	18,840	16,758	10,250	10,214	9,554
N bases ratio (%)	0.009137	0.009142	0.009041	0.009175	0.008854	0.008916
GC bases ratio (%)	50.71	50.28	50.91	51.12	50.71	51.29

Q20 bases ratio, the percentage of bases in the clean data with quality values greater than or equal to 20; Q30 bases ratio, the percentage of bases in the clean data with quality values greater than or equal to 30; N%, the percentage of undetermined bases in the clean data out of the total bases; GC bases ratio, the percentage of G and C bases out of the total bases.

Table 3. Statistics of sequencing read alignment

Sample	L01	L02	L03	L04	L05	L06
Total reads	168,319,300	204,605,264	184,167,668	110,986,482	114,567,750	106,287,400
Uniquely mapped reads	141,478,910	173,369,972	156,844,246	96,754,100	99,599,594	91,982,716
Percentage of uniquely mapped reads (%)	84.05	84.73	85.16	87.18	86.94	86.54
Multiple mapped reads	12,087,902	11,684,728	11,687,670	5,506,124	5,863,598	7,304,724
Percentage of multiple mapped (%)	7.18	5.71	6.35	4.96	5.12	6.87
Unmapped reads	13,110,782	16,796,230	13,586,796	7,551,296	7,800,662	6,355,936
Percentage of unmapped reads (%)	7.79	8.21	7.38	6.80	6.81	5.98
Overall alignment rate (%)	95.49	95.33	95.98	96.11	96.14	96.67

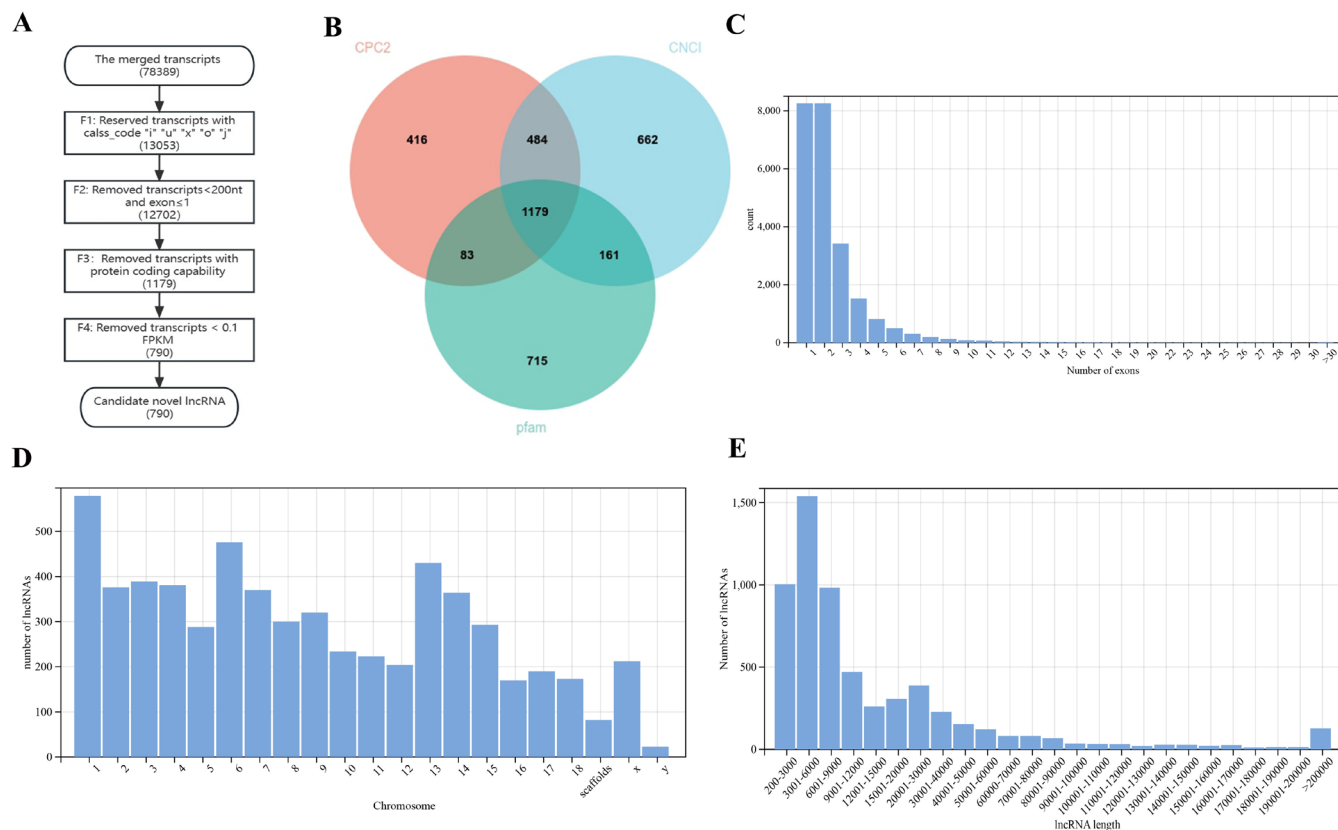


Figure 1. Screening of novel lncRNAs and genomic characterization of lncRNAs. (A) The flowchart of identifying novel lncRNA. (B) The Venn diagram of CPC2, CNCI and pfam software prediction. Pink represents CPC2, blue represents CNCI, green represents pfam. (C) Number of lncRNAs exons. (D) The chromosome distribution of lncRNAs. (E) Transcript length of lncRNAs.

Identification of differentially expressed lncRNAs

After differential expression analysis in the OS group and NC group, 79 DE lncRNAs (34 lncRNAs were upregulated and 45 lncRNAs were downregulated) were screened (Figure 2A; Supplementary Table S1). The heatmap showed that the expression levels of DE lncRNAs (Supplementary Table S2) were significantly different between the OS group and the NC group (Figure 2B).

Target gene prediction of DE lncRNA

Of the 79 DE lncRNAs, 61 lncRNAs had cis-target genes within 100,000 bp upstream and downstream, in a total of 135 targets. A total of 12,980 lncRNA-mRNA pairs were predicted to be associated by the Pearson correlation coefficient method. The top 50 lncRNA-mRNA gene pairs (Supplementary Table S3) with the most significant p-values were shown in Figure 2(C). In this figure, the DE lncRNAs point towards their target mRNAs, representing the differential expression of lncRNAs that regulated their target genes in trans.

Gene ontology enrichment analyses

In the present study, the target genes of DE lncRNAs were

significantly enriched in 68 BP, 40 CC, and 48 MF categories (Supplementary Table S4). The top 20 BP terms mainly included B-cell activation, cargo loading into COPII-coated vesicle, cell cycle, DNA recombination, regulation of growth, tissue development, and other terms (Figure 3A). The top 20 CC terms mainly included nucleus, cytosol, nucleoplasm, cytoplasm, kinetochore, chromatin, and other terms (Figure 3B). The top 20 MF mainly included RNA polymerase II core promoter proximal region sequence-specific DNA binding, chromatin binding, methyl-CpG binding, protein kinase A binding, and other terms (Figure 3C).

Kyoto encyclopedia of genes and genomes pathway analyses

A total of 4,645 target genes of DE lncRNAs were significantly enriched in 96 signaling pathways (Supplementary Table S5). The top 20 KEGG pathways mainly included metabolic pathways, cell cycle, chemical carcinogenesis-receptor activation, mismatch repair, DNA replication, chemical carcinogenesis-ROS, and other pathways (Figure 3D). Among the 96 KEGG pathways associated with OS were chemical carcinogenesis-ROS, colorectal cancer, Parkinson disease, insulin pathway, cellular senescence, Alzheimer's disease,

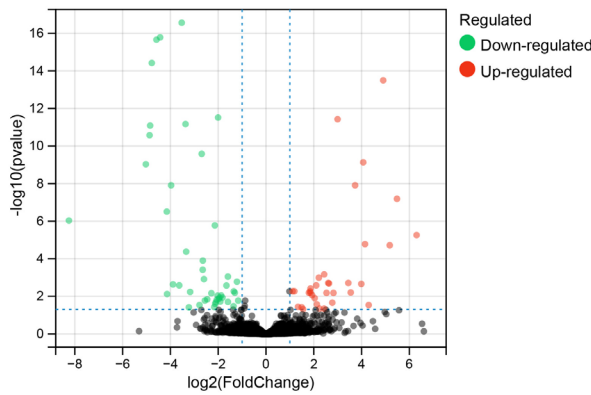
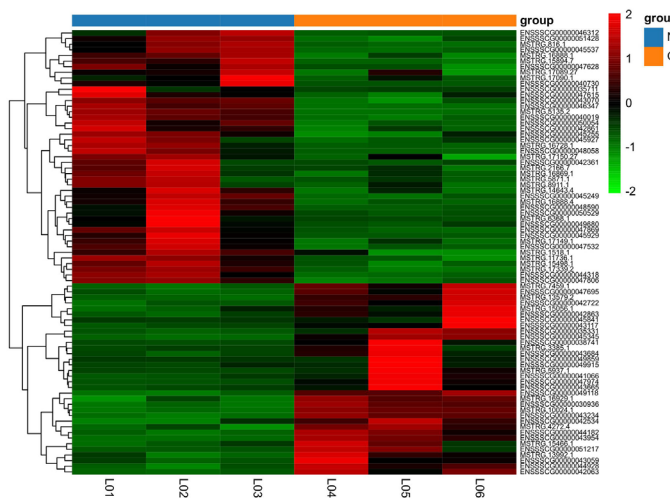
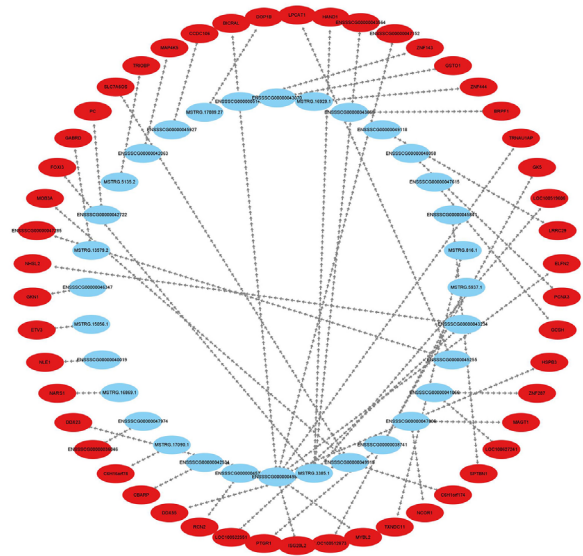
A

B

C


Figure 2. Statistics of DE lncRNAs and network. (A) Volcano plot analysis of 79 DE lncRNAs. The red dot represents the up-regulated gene, the green dot represents the down-regulated gene (B) Heatmap plots of DE lncRNAs. Rows represent lncRNAs, columns represent samples. The red color represents the higher expression of the gene in the sample and the green color represents the lower expression of the gene in the sample. (C) Interaction network for top 50 of lncRNA-mRNA gene pairs. The blue notes represent lncRNA. The red notes represent trans-target gene. DE, differentially expressed.

and other pathways.

Alternative splicing analysis

AS is an important mechanism of gene expression regulation, playing a crucial role in the normal functioning and disease development of organisms. In this research, a total of 12 AS events were detected (Figure 4). In this study, it was found alternative 5' first exon (TSS) and alternative 3' last exon (TTS) accounted for 67.84% to 72.13% of the AS events. This suggests that TSS and TTS were the two most prevalent AS events observed in this research.

Quantitative real-time polymerase chain reaction validation of the gene expression data from RNA-seq

To validate the accuracy of RNA-seq, six DE lncRNAs (three upregulated lncRNAs and three downregulated lncRNAs) were randomly selected to perform qRT-PCR (Figure 5A).

The correlation and p-value were obtained after linear fitting of the \log_2 (fold change). The results showed that there was a significant correlation between the RNA-seq and qRT-PCR ($r = 0.87$; $p = 0.03$ for DE lncRNAs) (Figure 5B). This also indicated the accuracy of high-throughput sequencing results.

DISCUSSION

As a vital organ, the intestine not only takes in nutrients but also stops harmful substances such as bacteria and endotoxins from getting through the intestinal wall and into the body's tissues, organs, and microcirculation [34]. Studies in the past have revealed that intraperitoneal injection of DQ can induce OS in piglets [35,36]. The DQ was thus used to construct a model of OS in piglets to study the effects of OS [37,38]. To further investigate the molecular mechanism of DQ-induced damage, RNA-Seq was used to identify DE lncRNAs. Over-

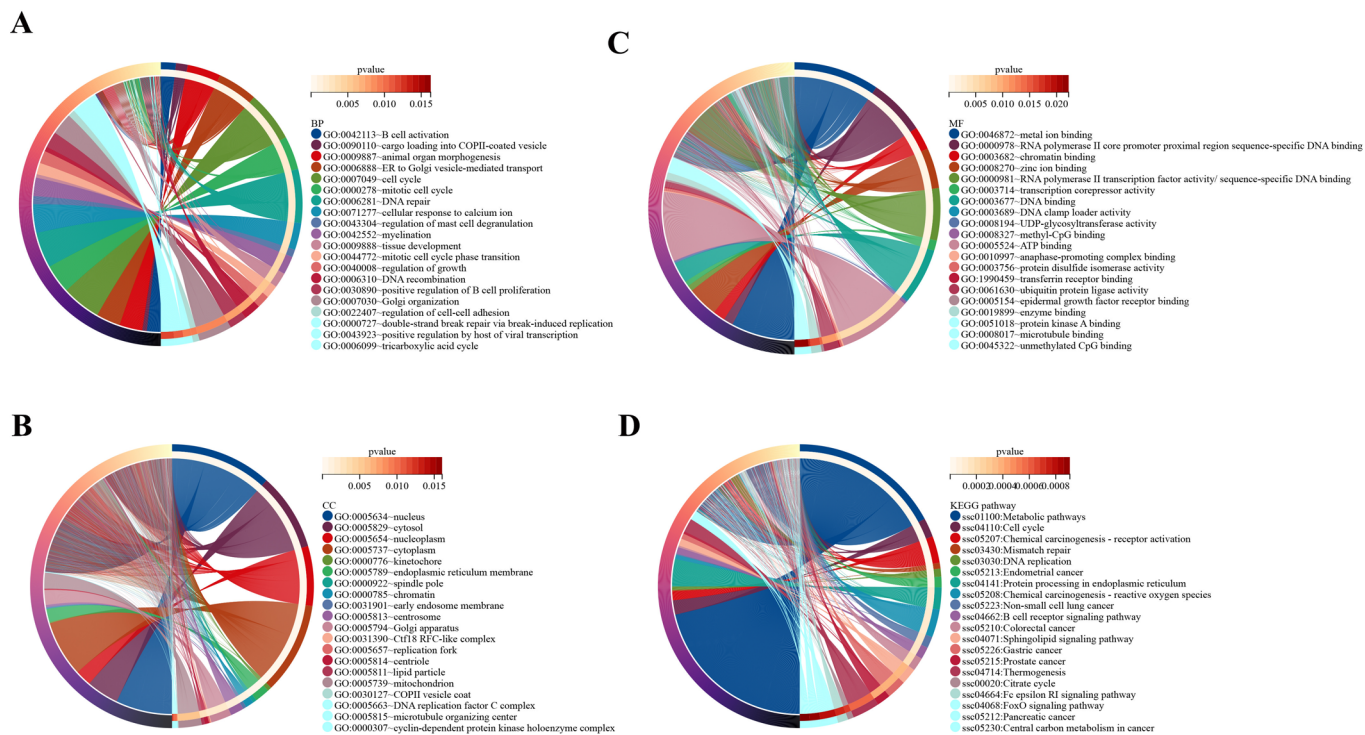


Figure 3. TOP 20 of GO enrichment analysis and KEGG pathways. In the circle diagram of GO enrichment and KEGG pathways, the circle is divided into a left half and a right half. In the left semicircle, the different colors represent different genes. In the outermost right semicircle, the different colors represent the different GO enrichments and KEGG pathways and the color of the inner side of the circle connected to the outermost side represents the p value, and the color changes from white to red as the p value increases. (A) Biological processes. (B) Cellular components. (C) Molecular functions. (D) KEGG pathways. GO, gene ontology; KEGG, Kyoto encyclopedia of genes and genomes.

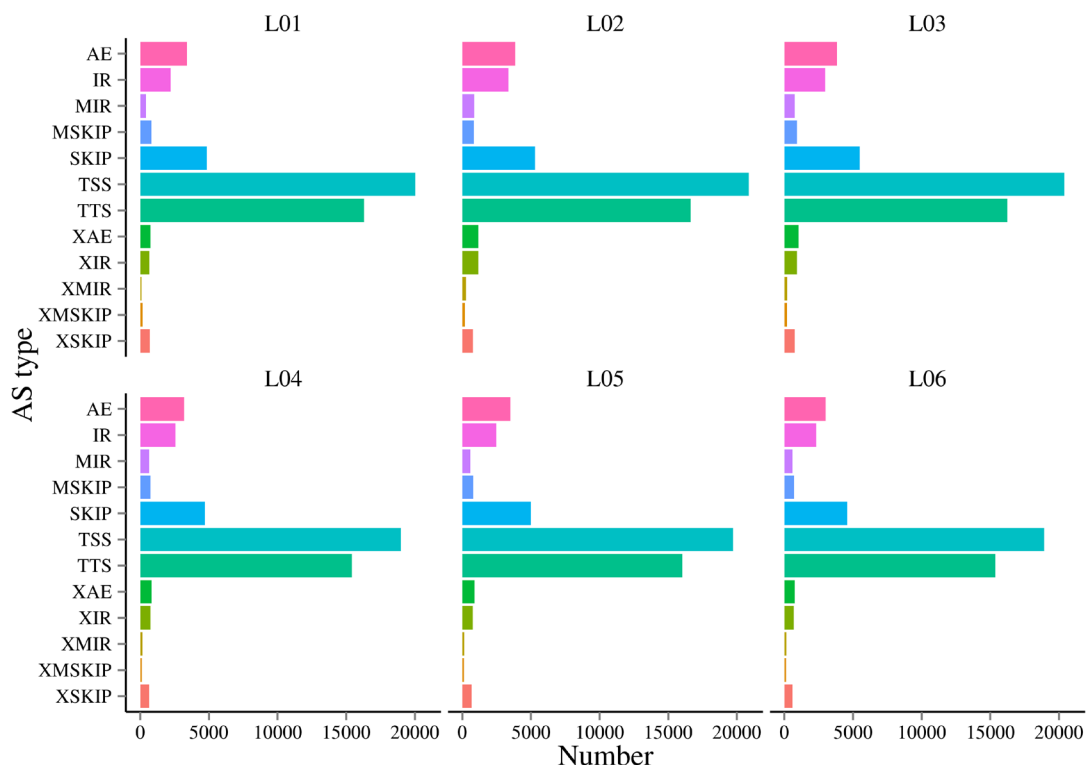


Figure 4. Statistics of AS events. The x-axis represents the quantity of AS events for each category. The y-axis represents the classification of AS events. Different colors show different types of AS events. AS, alternative splicing.

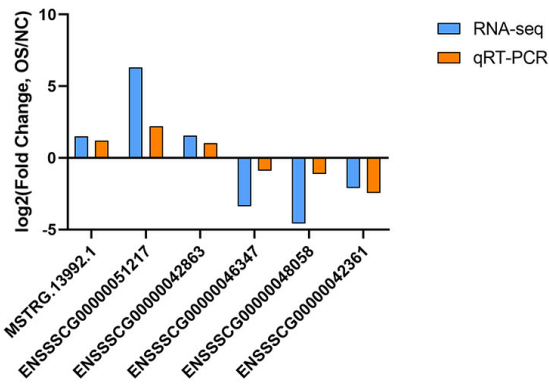
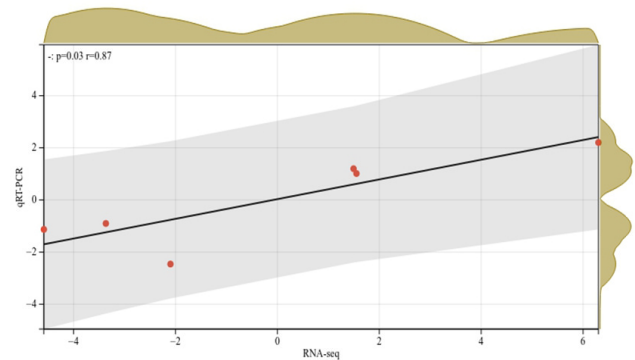
A

B


Figure 5. (A) Validation by qRT-PCR of 6 randomly selected DE lncRNAs from RNA-seq. (B) Correlation between RNA-seq and qRT-PCR. qRT-PCR, quantitative real-time polymerase chain reaction; DE, differentially expressed.

all, there were substantial variations in lncRNA expression in the jejunum between the OS and NC groups. Between the two groups, there were 79 DE lncRNAs.

lncRNAs have roles in a wide range of physiological and pathological processes, such as glucose and lipid metabolism [39], cancer [40], and skeletal muscle [41] function. Regardless of the BPs of lncRNAs, it is unknown whether lncRNAs function in the control of OS in the piglet jejunum. A total of 79 DE lncRNAs were discovered in our study. Although GO enrichment and KEGG pathway analyses did not reveal direct enrichment of antioxidant pathways, there were many pathways associated with OS, such as chemical carcinogenesis-ROS, colorectal cancer, Foxo pathway, AMPK pathway, and other pathways. Our research lays the groundwork for further study into the involvement of lncRNAs in DQ-induced OS.

Related research has reported that Foxo6 inhibits melanin formation in part by increasing intracellular antioxidant capacity [42] and suppressing ROS production [43]. In this study, the cis-target gene Foxo6 of the DE novel lncRNA MSTRG.13992.1 was enriched in the Foxo signal pathway. The lncRNA MSTRG.13992.1 was highly expressed in the OS group compared with the NC group. In conclusion, this finding predicts that the lncRNA MSTRG.13992.1 may prevent damage to the jejunum caused by OS from DQ.

OSU53, a novel AMPK activator, protects spinal cord nerves from OS caused by hydrogen peroxide (H_2O_2) through AMPK signaling pathways [44]. Through activation of AMPK, licochalcone D reduces OS-induced senescence [45]. SIRT1 is a deacetylase that affects gene expression by histone deacetylation. A research on SIRT1 revealed evidence of its function in reducing OS and inflammation [46]. The finding of this research revealed that SIRT1, the trans-target gene of lncRNA MSTRG.3385.1 and ENSSSCG00000049859, was enriched in AMPK signal pathway. Comparison of the expression levels

of MSTRG.3385.1 and ENSSSCG00000049859 between the OS and NC groups revealed that the OS group had higher expression of the lncRNA MSTRG.3385.1 and ENSSSCG00000049859. As the jejunum in the piglets was injected with DQ in the OS group, excessive free radicals were generated. Upregulation of the lncRNAs MSTRG.3385.1 and ENSSSCG00000049859, the trans-target genes of SIRT1, may have had a role in counteracting the excessive production of free radicals in the OS group. This finding indicates that the upregulation of MSTRG.3385.1 and ENSSSCG00000049859 may fight against OS in the jejunum.

Related studies have reported an association between OS and colorectal cancer. Excessive formation of ROS/RNS leads to OS, which is directly related to the progression of colorectal cancer [47,48]. The trans-target gene SOS1 of the lncRNA MSTRG.5871.1 and ENSSSCG00000042361 was enriched in the colorectal cancer pathway. Compared with the NC group, the OS group exhibited lower expression of the lncRNA MSTRG.5871.1 and ENSSSCG00000042361. For colorectal cancer, this predicts that the downregulation of MSTRG.5871.1 and ENSSSCG00000042361 may provide a viable treatment option. This study's finding supports previous research in which SOS1 degraders were deemed to be feasible therapeutic agents for KRAS-mutant colorectal cancer [49].

CONCLUSION

In conclusion, this research discovered that DQ-induced OS caused a difference in the expression of lncRNAs in the jejunum in piglets. In brief, 79 DE lncRNAs were identified. The target genes of the DE lncRNAs were enriched in pathways related to OS. Therefore, there DE lncRNAs were found to have crucial functions in OS. Additionally, our findings establish a solid basis for future research into oxidative-induced pathological processes.

CONFLICT OF INTEREST

We certify that there is no conflict of interest with any financial organization regarding the material discussed in the manuscript.

FUNDING

This study was supported by Shandong Provincial Natural Science Foundation (ZR2022QC075), Shandong “Double Tops” Program (SYL2017YSTD12), and Shandong Province Pig Industry Technology System Project (SDAIT-08-02).

SUPPLEMENTARY MATERIAL

Supplementary file is available from: <https://doi.org/10.5713/ab.23.0202>

Supplementary Table S1. The list of differentially expressed lncRNAs

Supplementary Table S2. The expression of differentially expressed lncRNAs

Supplementary Table S3. Top 50 of lncRNA-mRNA gene pairs

Supplementary Table S4. GO enrichment analyses of target genes of DE-lncRNAs

Supplementary Table S5. KEGG pathways of target genes of DE lncRNAs

REFERENCES

- Sies H. Oxidative stress: a concept in redox biology and medicine. *Redox Biol* 2015;4:180-3. <https://doi.org/10.1016/j.redox.2015.01.002>
- Li Z, Bi R, Sun S, et al. The role of oxidative stress in acute ischemic stroke-related thrombosis. *Oxid Med Cell Longev* 2022;2022:8418820. <https://doi.org/10.1155/2022/8418820>
- Srinivas US, Tan BWQ, Vellayappan BA, Jeyasekharan AD. ROS and the DNA damage response in cancer. *Redox Biol* 2019;25:101084. <https://doi.org/10.1016/j.redox.2018.10.1084>
- Burton GJ, Jauniaux E. Oxidative stress. *Best Pract Res Clin Obstet Gynaecol* 2011;25:287-99. <https://doi.org/10.1016/j.bpobgyn.2010.10.016>
- Aw TY. Intestinal glutathione: determinant of mucosal peroxide transport, metabolism, and oxidative susceptibility. *Toxicol Appl Pharmacol* 2005;204:320-8. <https://doi.org/10.1016/j.taap.2004.11.016>
- Luissint A, Parkos CA, Nusrat A. Inflammation and the intestinal barrier: leukocyte-epithelial cell interactions, cell junction remodeling, and mucosal repair. *Gastroenterology* 2016;151:616-32. <https://doi.org/10.1053/j.gastro.2016.07.008>
- Zheng P, Yu B, He J, et al. Protective effects of dietary arginine supplementation against oxidative stress in weaned piglets. *Br J Nutr* 2013;109:2253-60. <https://doi.org/10.1017/S0007114512004321>
- Cao S, Wu H, Wang C, et al. Diquat-induced oxidative stress increases intestinal permeability, impairs mitochondrial function, and triggers mitophagy in piglets. *J Anim Sci* 2018;96:1795-805. <https://doi.org/10.1093/jas/sky104>
- Amaral PP, Dinger ME, Mattick JS. Non-coding RNAs in homeostasis, disease and stress responses: an evolutionary perspective. *Brief Funct Genomics* 2013;12:254-78. <https://doi.org/10.1093/bfgp/elt016>
- Ma Q. Transcriptional responses to oxidative stress: pathological and toxicological implications. *Pharmacol Ther* 2010;125:376-93. <https://doi.org/10.1016/j.pharmthera.2009.11.004>
- Bonasio R, Shiekhattar R. Regulation of transcription by long noncoding RNAs. *Annu Rev Genet* 2014;48:433-55. <https://doi.org/10.1146/annurev-genet-120213-092323>
- Quinodoz S, Guttman M. Long noncoding RNAs: an emerging link between gene regulation and nuclear organization. *Trends Cell Biol* 2014;24:651-63. <https://doi.org/10.1016/j.tcb.2014.08.009>
- Fatica A, Bozzoni I. Long non-coding RNAs: new players in cell differentiation and development. *Nat Rev Genet* 2014;15:7-21. <https://doi.org/10.1038/nrg3606>
- Tehrani SS, Karimian A, Parsian H, Majidinia M, Yousefi B. Multiple functions of long non-coding RNAs in oxidative stress, DNA damage response and cancer progression. *J Cell Biochem* 2018;119:223-36. <https://doi.org/10.1002/jcb.26217>
- Gao Q, Zhang C, Li JX, et al. Melatonin attenuates H₂O₂-induced oxidative injury by upregulating lncRNA NEAT1 in HT22 hippocampal cells. *Int J Mol Sci* 2022;23:12891. <https://doi.org/10.3390/ijms232112891>
- Xie W, Shu T, Peng H, et al. lncRNA h19 inhibits oxidative stress injury of cochlear hair cells by regulating mir-653-5p/sirt1 axis. *Acta Biochim Biophys Sin (Shanghai)* 2022;54:332-9. <https://doi.org/10.3724/abbs.2022018>
- Magalhaes N, Carvalho F, Dinis-Oliveira RJ. Human and experimental toxicology of diquat poisoning: toxicokinetics, mechanisms of toxicity, clinical features, and treatment. *Hum Exp Toxicol* 2018;37:1131-60. <https://doi.org/10.1177/0960327118765330>
- Li Z, Chen W, Qin M, Wang L, Zeng Y. Characteristics of circRNAs expression profiles in the piglets intestine induced by oxidative stress. *Genes Genomics* 2022;44:425-33. <https://doi.org/10.1007/s13258-021-01154-4>
- Chen S, Zhou Y, Chen Y, Gu J. Fastq: an ultra-fast all-in-one fastq preprocessor. *Bioinformatics* 2018;34:i884-90. <https://doi.org/10.1093/bioinformatics/bty560>
- Kim D, Langmead B, Salzberg SL. HISAT: a fast spliced aligner with low memory requirements. *Nat Methods* 2015;12:357-60. <https://doi.org/10.1038/nmeth.3317>
- Pertea M, Pertea GM, Antonescu CM, Chang TC, Mendell JT, Salzberg SL. StringTie enables improved reconstruction of a transcriptome from RNA-seq reads. *Nat Biotechnol* 2015;

- 33:290-5. <https://doi.org/10.1038/nbt.3122>
22. Liao Y, Smyth GK, Shi W. Featurecounts: an efficient general purpose program for assigning sequence reads to genomic features. *Bioinformatics* 2014;30:923-30. <https://doi.org/10.1093/bioinformatics/btt656>
 23. Pertea G, Pertea M. Gff utilities: gffread and gffcompare [version 2; Peer review: 3 approved]. *F1000Res* 2020;9:304. <https://doi.org/10.12688/f1000research.23297.2>
 24. Kang Y, Yang D, Kong L, et al. Cpc2: a fast and accurate coding potential calculator based on sequence intrinsic features. *Nucleic Acids Res* 2017;45:W12-6. <https://doi.org/10.1093/nar/gkx428>
 25. Sun L, Luo H, Bu D, et al. Utilizing sequence intrinsic composition to classify protein-coding and long non-coding transcripts. *Nucleic Acids Res* 2013;41:e166. <https://doi.org/10.1093/nar/gkt646>
 26. Mistry J, Chuguransky S, Williams L et al. Pfam: the protein families database in 2021. *Nucleic Acids Res* 2021;49:D412-9. <https://doi.org/10.1093/nar/gkaa913>
 27. Love MI, Huber W, Anders S. Moderated estimation of fold change and dispersion for rna-seq data with *deseq2*. *Genome Biol* 2014;15:550. <https://doi.org/10.1186/s13059-014-0550-8>
 28. Quinlan AR, Hall IM. *Bedtools*: a flexible suite of utilities for comparing genomic features. *Bioinformatics* 2010;26:841-2. <https://doi.org/10.1093/bioinformatics/btq033>
 29. Venkatesan A, Barik A, Paul D, Muthaiyan M, Das R. Identification of novel lncrna by reanalysis of rna-seq data in zika virus infected hinpccs. *Virusdisease* 2022;33:185-93. <https://doi.org/10.1007/s13337-022-00771-1>
 30. Mukaka MM. Statistics corner: a guide to appropriate use of correlation coefficient in medical research. *Malawi Med J* 2012;24:69-71.
 31. Sherman BT, Hao M, Qiu J, et al. David: a web server for functional enrichment analysis and functional annotation of gene lists (2021 update). *Nucleic Acids Res* 2022;50:W216-21. <https://doi.org/10.1093/nar/gkac194>
 32. Florea L, Song L, Salzberg SL. Thousands of exon skipping events differentiate among splicing patterns in sixteen human tissues. *F1000Res* 2013;2:188. <https://doi.org/10.12688/f1000research.2-188.v2>
 33. Schmittgen TD, Livak KJ. Analyzing real-time pcr data by the comparative ct method. *Nat Protoc* 2008;3:1101-8. <https://doi.org/10.1038/nprot.2008.73>
 34. Gou HZ, Zhang YL, Ren LF, et al. How do intestinal probiotics restore the intestinal barrier? *Front Microbiol* 2022;13:929346. <https://doi.org/10.3389/fmicb.2022.929346>
 35. Li Z, Chen W, Qin M, Wang L, Zeng Y. Characteristics of circrnas expression profiles in the piglets intestine induced by oxidative stress. *Genes Genomics* 2022;44:425-33. <https://doi.org/10.1007/s13258-021-01154-4>
 36. Wang J, Li Z, Yang D, et al. Diquat determines a deregulation of lncrna and mrna expression in the liver of postweaned piglets. *Oxid Med Cell Longev* 2019;2019:9148535. <https://doi.org/10.1155/2019/9148535>
 37. Yuan S, Chen D, Zhang K, Yu B. Effects of oxidative stress on growth performance, nutrient digestibilities and activities of antioxidative enzymes of weanling pigs. *Asian-Australas J Anim Sci* 2007;20:1600-5. <https://doi.org/10.5713/ajas.2007.1600>
 38. Zheng P, Yu B, Lv M, Chen D. Effects of oxidative stress induced by diquat on arginine metabolism of postweaning pigs. *Asian-Australas J Anim Sci* 2010;23:98-105. <https://doi.org/10.5713/ajas.2010.90270>
 39. Zhang TN, Wang W, Yang N, et al. Regulation of glucose and lipid metabolism by long non-coding rnas: facts and research progress. *Front Endocrinol (Lausanne)* 2020;11:457. <https://doi.org/10.3389/fendo.2020.00457>
 40. Wang S, Chen Z, Gu J, Chen X, Wang Z. The role of lncrna pcat6 in cancers. *Front Oncol* 2021;11:701495. <https://doi.org/10.3389/fonc.2021.701495>
 41. Ma L, Qin M, Zhang Y, et al. Identification and functional prediction of long non-coding rnas related to skeletal muscle development in duroc pigs. *Anim Biosci* 2022;35:1512-23. <https://doi.org/10.5713/ab.22.0020>
 42. Moon KM, Lee B, Kim DH, HY Chung. Foxo6 inhibits melanogenesis partly by elevating intracellular antioxidant capacity. *Redox Biol* 2020;36:101624. <https://doi.org/10.1016/j.redox.2020.101624>
 43. Bang E, Kim DH, Chung HY. Protease-activated receptor 2 induces ros-mediated inflammation through akt-mediated nf-kb and foxo6 modulation during skin photoaging. *Redox Biol* 2021;44:102022. <https://doi.org/10.1016/j.redox.2021.102022>
 44. Xu J, Wu L, Zhang Y, et al. Activation of ampk by osu53 protects spinal cord neurons from oxidative stress. *Oncotarget* 2017;8:112477-86. <https://doi.org/10.18632/oncotarget.22055>
 45. Maharajan N, Ganesan CD, Moon C, Jang CH, Oh WK, Cho GW. Licochalcone d ameliorates oxidative stress-induced senescence via ampk activation. *Int J Mol Sci* 2021;22:7324. <https://doi.org/10.3390/ijms22147324>
 46. Singh V, Ubaid S. Role of silent information regulator 1 (sirt1) in regulating oxidative stress and inflammation. *Inflammation* 2020;43:1589-98. <https://doi.org/10.1007/s10753-020-01242-9>
 47. Basak D, Uddin MN, Hancock J. The role of oxidative stress and its counteractive utility in colorectal cancer (crc). *Cancers (Basel)* 2020;12:3336. <https://doi.org/10.3390/cancers12113336>
 48. Carini F, Mazzola M, Rappa F, et al. Colorectal carcinogenesis: role of oxidative stress and antioxidants. *Anticancer Res* 2017;37:4759-66. <https://doi.org/10.21873/anticancer.11882>
 49. Bian Y, Alem D, Beato F, et al. Development of sos1 inhibitor-based degraders to targetkras-mutant colorectal cancer. *J Med Chem* 2022;65:16432-50. <https://doi.org/10.1021/acs.jmedchem.2c01300>